Effect of Pt doping on the critical temperature and the upper critical field in $YNi_{2-x}Pt_xB_2C$ for doping range $0<x<0.2$

Sourin Mukhopadhyay,[1] Goutam Sheet,[1,*] A. K. Nigam,[1] Pratap Raychaudhuri,[1,†] and H. Takeya[2]
[1]*Department of Condensed Matter Physics and Materials Science, Tata Institute of Fundamental Research, Homi Bhabha Road, Colaba, Mumbai 400005, India*
[2]*National Institute of Materials Science, 3-13 Sakura, Tsukuba, Ibaraki 305-0003, Japan*
(Received 26 September 2008; revised manuscript received 19 December 2008; published 22 April 2009)

We investigate the evolution of superconducting properties by doping nonmagnetic impurity in single crystals of $YNi_{2-x}Pt_xB_2C$ ($x=0-0.2$). With increasing Pt doping the critical temperature (T_c) monotonically decreases from 15.85 K and saturates to a value of ~13 K for $x\geq 0.14$. However, unlike usual *s*-wave superconductors, the upper critical field (H_{c2}) along both crystallographic directions *a* and *c* decreases with increasing Pt doping. Specific-heat measurements show that the density of states [$N(E_F)$] at the Fermi level (E_F) and the Debye temperatures (Θ_D) in this series remain constant within the error bars of our measurement. We explain our results based on the increase in interband scattering in the multiband superconductor YNi_2B_2C.

DOI: 10.1103/PhysRevB.79.132505 PACS number(s): 74.25.Op, 74.70.Dd, 74.62.−c

There has been an increase in interest in multiband superconductors in recent years after the clear elucidation of multiband superconductivity[1] in MgB_2 arising from the π and σ bands. The simplest form of multiband superconductivity arises when electrons on different Fermi sheets in the same metal have different electron-phonon coupling strength, leading to different sheets on the Fermi surface exhibiting different superconducting energy gaps (Δ). When the sample is in the clean limit, spectroscopic measurements on such a system reveal different superconducting energy gaps and different superconducting transition temperatures (T_c) on different Fermi sheets. Of particular interest in multiband superconductors is the evolution of the superconducting properties when one drives the system toward the dirty limit by substituting with nonmagnetic impurities. In a conventional *s*-wave superconductor, nonmagnetic disorder results in an increase in electronic scattering rate which decreases the electronic mean-free path (l) and the coherence length (ξ). This results in an increase in the upper critical field[2] (H_{c2}). The T_c on the other hand is not affected by nonmagnetic impurities[3] unless the impurities result in a modification of the electronic or lattice properties, e.g., density of states at Fermi level [$N(E_F)$] or the Debye temperature (Θ_D). In contrast, the situation in multiband superconductors is more complicated. For multiband superconductors in the clean limit, the band with strongest electron-phonon coupling governs the bulk properties such as T_c and H_{c2}. Substitution of nonmagnetic impurities results in intraband scattering of electrons on individual Fermi sheets as well as interband scattering of electrons between different Fermi sheets. The former has an effect similar to conventional superconductor for individual bands, whereas the latter causes the bulk properties to be governed in the dirty limit by an average property of all the electrons instead of being governed by those with strongest electron-phonon coupling strength. Therefore, the evolution of T_c and H_{c2} for a multiband superconductor with the substitution of nonmagnetic impurities is governed by a complex interplay[4,5] of interband and intraband scatterings. In particular, H_{c2} need not necessarily increase with an increase in electronic scattering. The evolution of H_{c2} in a multiband superconductor with impurity is therefore a matter of considerable interest.

In this Brief Report, we study the evolution of T_c and H_{c2} in a series of Pt-doped YNi_2B_2C single crystals, e.g., $YNi_{2-x}Pt_xB_2C$ ($x=0-0.2$). The quaternary borocarbide superconductor[6] YNi_2B_2C displays several unusual properties, namely, large anisotropy in the superconducting order parameter,[7–9] a positive curvature[10] in $H_{c2}(T)$ close to T_c, and a square flux-line lattice[11] at high magnetic fields. In a previous paper,[12] through measurements of Δ along different crystallographic directions using directional point-contact spectroscopy (DPCS), we have shown that these unusual properties can be understood from a multiband scenario, where large difference in the Fermi velocity on different Fermi sheets[13] gives rise to different electron-phonon coupling strength and different values of Δ. In this Brief Report, we carry out a detailed measurements of H_{c2} by applying magnetic field along the two crystallographic directions *a* and *c*. The central observations of this Brief Report are the following: (i) with increasing *x*, both T_c and H_{c2} measured along the two crystallographic directions *a* and *c* decreases and saturates for $x\geq 0.14$ and (ii) the anisotropy in H_{c2} (for $H\|a$ and $H\|c$) decreases monotonically with increasing *x*. Measurement of specific heat reveals that $N(E_F)$ and Θ_D does not change significantly within the error bars of our measurements. Our results elucidate the role of nonmagnetic impurity in a multiband scenario where the increase in interband scattering dominates over the increase in intraband scattering.

Single crystals of $YNi_{2-x}Pt_xB_2C$ ($x=0.02$, 0.06, 0.1, 0.14, and 0.2) were grown by the traveling-solvent floating-zone method using an image furnace. X-ray powder diffraction using the crushed $YNi_{2-x}Pt_xB_2C$ single crystals was performed to determine the lattice parameters. X-ray profiles were analyzed through Rietveld refinement using the FULLPROF program. A homemade high frequency (15 KHz) planar coil ac susceptibility setup was used to determine the critical temperatures (T_c) of these samples. The critical fields (H_{c2}) along two crystallographic directions *a* and *c* was determined from isothermal measurements of $\chi'(H)$ as a function of H

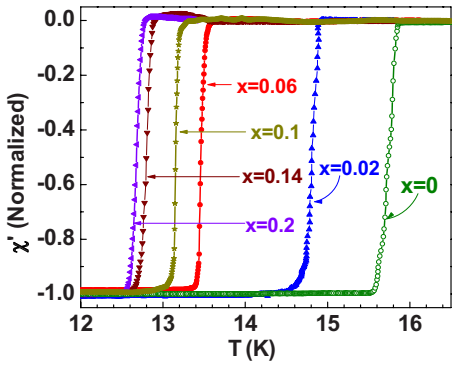

FIG. 1. (Color online) Normalized real part of ac susceptibility (χ') as a function of temperature (T) in $YNi_{2-x}Pt_xB_2C$ for $x=0-0.2$. Solid lines are a guide for the eyes.

using the same setup down to 2.2 K and magnetic fields up to 8.5 T. For the undoped YNi_2B_2C sample the H_{c2} for $H\|a$ was larger than the maximum magnetic field of our ac susceptibility cryostat. This value was therefore obtained from a separate measurement of the isothermal magnetization versus field (M-H) loop at 2.2 K up to 12 T using an Oxford Instrument vibrating sample magnetometer. Specific-heat measurements in the superconducting and normal state were carried out in a Quantum Design physical properties measurement system at zero field and at 9 T, respectively, over the temperature range of 2–25 K.

X-ray diffraction analysis reveals that pure YNi_2B_2C has tetragonal lattice structure with lattice parameters $a=3.52$ Å and $c=10.54$ Å. With Pt doping the lattice parameters along both a and c axes increase monotonically, and for $x=0.2$ the lattice constants along [100] and [001] become 3.54 Å and 10.62 Å, respectively. The increase in the volume of the unit cell in the range $x=0-0.2$ is ~1.1%. Thus, there is a continuous incorporation of Pt on Ni sites without significant change in the atomic distances and the structural anisotropy.[14] Figure 1 shows the normalized real part of ac susceptibility (χ') as a function of temperature for all the samples. The T_c is determined from the onset of superconducting transition, defined as 5% of the full signal change in the real part of ac susceptibility [$\chi'(T)$]. For the undoped YNi_2B_2C, $T_c \sim 15.85$ K. With increased incorporation of Pt, T_c decreases monotonically; T_c falls sharply from 15.85 K ($x=0$) to 13.6 K ($x=0.06$) and then decreases gradually to 12.75 K in the range $x=0.06-0.2$. Figure 2 shows $H_{c2\|a}$ and $H_{c2\|c}$ extracted from the field variation in $\chi'(H)$ for all the six samples as a function of temperature. The variation in $\chi'(H)$ with magnetic field at 2.2 K is shown in the *insets* for both $H\|a$ and $H\|c$. Almost all the $\chi'(H)$-H graph shows a pronounced "peak effect"[15] [dip in $\chi'(H)$] just before H_{c2} arises from the order-disorder transition of the vortex lattice. The H_{c2} values at different temperatures are determined from the $\chi(T)$-H data [inset of Figs. 2(a)–2(f)] using the same criterion as fixed to extract the T_c values. To check the consistency of this procedure of extracting $H_{c2}(T)$, we have also compared the $H_{c2}(T)$ determined from isothermal M-H measurements[16] for the sample with $x=0.2$. The two curves are identical within the error bar of our measurement. We find a large anisotropy in the undoped YNi_2B_2C single crystal with[17,18] $\gamma_H = H_{C2\|a}/H_{C2\|c} \sim 1.18$. In pure YNi_2B_2C at 2.2 K, $H_{c2\|c} \sim 8.25$ T and $H_{c2\|a} \sim 9.77$ T.[19] With an increase in Pt, $H_{c2}(T)$ decreases in both directions.[20] The variation in T_c, $H_{c2\|a}$ and $H_{c2\|c}$ (at 2.2 K), as a function of x is shown in Fig. 3. The anisotropy decreases from $\gamma_H \approx 1.18$ for the undoped sample to $\gamma_H \approx 1$ for the sample with $x=0.2$ (inset of Fig. 3).

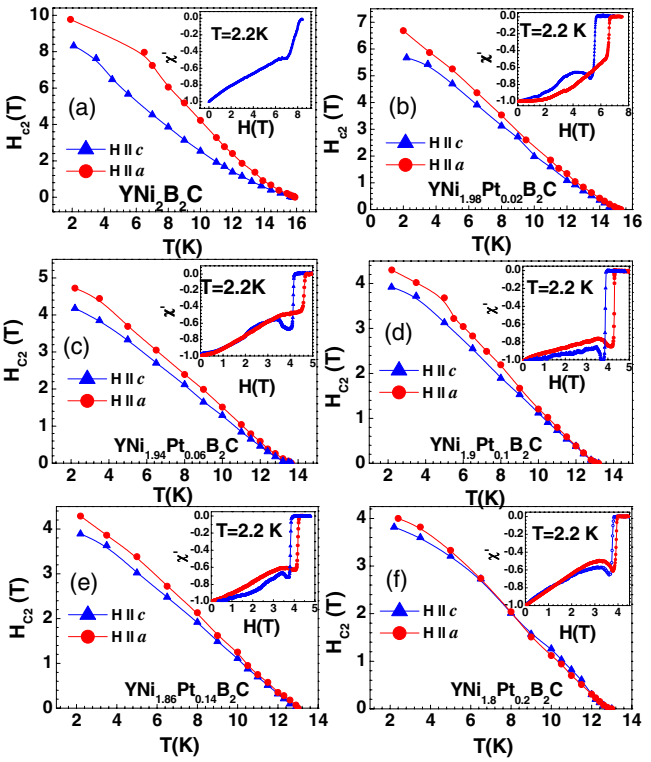

FIG. 2. (Color online) (a)-(f) Variation in H_{c2} with T along $H\|a$ and $H\|c$ for $YNi_{2-x}Pt_xB_2C$ with $x=0-0.2$. Solid lines are a guide for the eyes. The insets show variation in normalized $\chi'(H)$ with magnetic field (H) at 2.2 K for the same. All crystals show a pronounced peak effect close to H_{c2}. The H_{c2} value at 2.2 K for $H\|a$ in the undoped YNi_2B_2C is determined from isothermal magnetization versus field measurements.

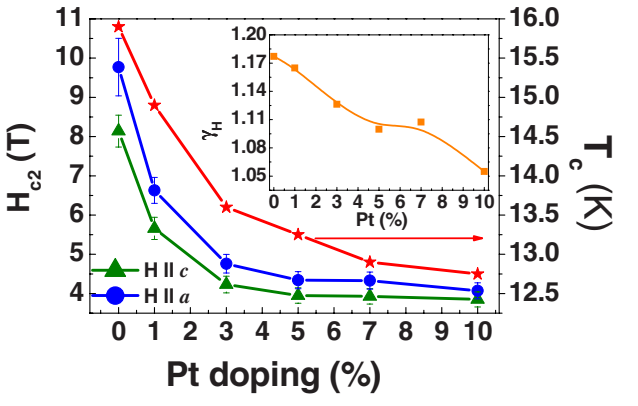

FIG. 3. (Color online) Variation in H_{c2} at 2.2 K with Pt doping in $YNi_{2-x}Pt_xB_2C$ in the range $x=0-0.2$, for both $H\|a$ (blue, solid circle) and $H\|c$ (green, solid triangle). The red line (star) shows the variation in T_c with the same Pt doping. Inset shows the variation in $\gamma_H = H_{c2\|a}/H_{c2\|c}$ at 2.2 K for the same. Solid lines are a guide for the eyes.

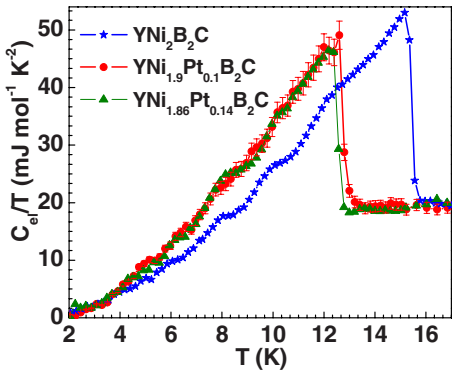

FIG. 4. (Color online) Temperature (T) dependence of electronic specific heat (C_{el}) plotted as C_{el}/T vs T for $YNi_{2-x}Pt_xB_2C$ with $x=0$, 0.1, and 0.14. Solid lines are a guide for the eyes. Representative error bars are shown on the $x=0.1$ sample.

The rapid decrease in H_{c2} in YNi_2B_2C upon substitution of Pt impurities is clearly not consistent with a conventional scenario. However, since the Fermi surface of YNi_2B_2C is very anisotropic we first compare the results with that of a single band superconductor with anisotropic Fermi surface. For a single band superconductor with anisotropic[2] Fermi surface in the clean limit,

$$H_{c2}\|c=\frac{\Phi_0}{2\pi(\xi_{0_{ab}})^2}=\frac{\Phi_0\pi\Delta^2}{2\hbar^2(v_{F_{ab}})^2}, \tag{1}$$

$$H_{c2}\|a=\frac{\Phi_0}{2\pi\xi_{0_a}\xi_{0_c}}=\frac{\Phi_0\pi\Delta^2}{2\hbar^2 v_{F_a}v_{F_c}}, \tag{2}$$

$$\gamma_H=\frac{v_{F_{ab}}}{v_{F_c}}, \tag{3}$$

where Φ_0 is the flux quantum and v_{F_a} and v_{F_c} are the Fermi velocities in the two directions (we assume $v_a=v_b=v_{ab}$ and $\xi_a=\xi_b=\xi_{ab}$ consistent with the tetragonal symmetry of the system). The anisotropy for such a superconductor, γ_H, would gradually decrease with increased intraband scattering. However, the average value of the critical fields, $H_{c2}\|a$ and $H_{c2}\|c$ ($\langle H_{c2}\rangle$), would show an increase due to reduction in electronic mean-free path. In contrast, in YNi_2B_2C, in addition to the decrease in the individual values of $H_{c2\|a}$ and $H_{c2\|c}$, $\langle H_{c2}\rangle$ decreases with an increase in Pt doping to almost half its value in the clean limit.

To verify whether this evolution of H_{c2} results from a change[21] in $N(E_F)$ or Θ_D upon substitution of Pt at the Ni site, we measured the specific heat (C_p) on the samples with $x=0$, 0.1, and 0.14. For all three samples measurements are carried out at $H=0$ and at $H=9$ T ($H\|c$), where the superconductivity is suppressed. Fitting the expression for the normal-state specific heat,[22] $C_n(T)=\gamma_nT+\beta T^3+\alpha T^5$ (where $C_{electronic}=\gamma_nT$ and $C_{lattice}(T)=\beta T^3+\alpha T^5$ with the C_p measured at 9 T, the lattice contribution, $C_{lattice}(T)$, is evaluated. Since $C_{lattice}(T)$ is independent of magnetic field, the electronic specific heat (C_{el}) at $H=0$ is determined by subtracting the phonon contribution from the measured C_p at $H=0$. Figure 4 shows the C_{el}/T vs T for three samples. It is clear that C_{el} in the normal state does not change significantly showing that $N(E_F)$ is not affected by Pt doping. The extracted value of γ_n and Θ_D for the three samples are (i) $\gamma_n=19\pm0.5$ mJ/mol K^2 and $\Theta_D=507\pm15$ K for $x=0$; (ii) $\gamma_n=20.1\pm0.5$ mJ/mol K^2 and $\Theta_D=522\pm15$ K for $x=0.1$; (iii) $\gamma_n=19.2\pm0.5$ mJ/mol K^2 and $\Theta_D=523\pm15$ K for $x=0.14$. Though we could not measure the specific heat of the other composition due to the small mass of the crystals, within the error bars of our measurements, γ_n remains constant with Pt doping[23,24] whereas Θ_D only shows a marginal increase. Therefore, the variation H_{c2} in $YNi_{2-x}Pt_xB_2C$ has to be analyzed beyond the single band scenario.

To understand the variation in H_{c2} with Pt doping we have to take into account the multiband nature of superconductivity in YNi_2B_2C. Spectroscopic measurements using DPCS on YNi_2B_2C single crystals[12] in the clean limit revealed the presence of at least two groups of electrons on two different Fermi sheets, for which the superconducting energy gap and T_c vary by a factor of 5–6. Comparison with band-structure calculations[13] indicates that the first group of electrons are on a "square-pancake" Fermi sheet (SPFS), whereas the second group of electrons are on a cylindrical Fermi sheet (CFS). In the clean limit, the bulk T_c coincides with the first group of electrons with higher T_c. DPCS studies in the clean system indicates that H_{c2} is also determined by the electrons on the square-pancake Fermi sheet[4,12] since the superconductivity on the other Fermi sheet is rapidly suppressed under the application of a magnetic field. Since the square-pancake Fermi sheet is very anisotropic, for the clean system without significant interband scattering, the $H_{c2}(0)$ will be given by Eqs. (1) and (2) where Δ and v_{Fab} and v_{Fc} have to be replaced by the ones corresponding to the square-pancake Fermi sheet. The anisotropy, γ_H, in the undoped compound thus reflects the anisotropy of the square-pancake Fermi sheet for which $v_{F_{ab}}>v_{F_c}$. This value is however much smaller than the ratio $v_{F_{ab}}/v_{F_c}>5$ estimated for this Fermi sheet from electronic structure[13] calculations. This indicates that even the undoped system individual bands are already in the "dirty" limit with significant intraband scattering, which decreases the H_{c2} anisotropy expected in a clean system. In such a system, addition of impurities would result[5] (i) in an increase in intraband scattering within each Fermi Sheet and (ii) in an increase in interband scattering between the two Fermi sheets. The first effect, which is expected to be small since the intraband scattering is already large in the parent material, will, in principle, increase the bulk H_{c2} governed by the coherence length of the electrons on the square-pancake Fermi sheet. The second effect would decrease the superconducting energy gap (and H_{c2}) on the square pancake due to the influence of the cylindrical Fermi sheet. The rapid decrease in $\langle H_{c2}\rangle$ with an increase in Pt doping suggests that that the second effect dominates over the first one in the doping range of this study. The large increase in interband scattering can be understood from the fact that both the square-pancake Fermi sheet and the cylindrical Fermi sheet have large contribution from the Ni $3d$ band. Therefore, Pt doping at the Ni site is likely to increase the interband scattering between these two Fermi sheets. At the same time γ_H decreases with increasing x due to the decrease in anisotropy of individual

bands. This decrease is however small since the individual bands already have significant intraband scattering in the parent compound.

Finally, we would like to note that the variation in T_c with Pt doping can be understood from the same mechanism. With an increase in interband scattering, the T_c will gradually decrease due to the influence of the second group of electrons[25] with lower T_c and will go toward a limiting value given by the weighted average of the T_c of the two bands. The rapid decrease in T_c at small values of x and the subsequent leveling off for $x>0.14$ supports this scenario.

In summary, we have investigated the effect of impurities on H_{c2} by studying a series of $YNi_{2-x}Pt_xB_2C$ single crystals. We show that both $H_{c2}\|a$ and $H_{c2}\|c$ and the T_c decreases with increasing x. Our results can be understood within a multiband scenario where the dominant contribution comes from the increase in interband scattering arising from Pt impurities. The relative insensitivity of H_{c2} and T_c for $x>0.14$ suggests that at large doping $YNi_{2-x}Pt_xB_2C$ behaves as an effective single band superconductor due to large interband scattering. This study elucidates the role of interband scattering on the upper critical field in a multiband superconductor and reinforces the multiband nature of superconductivity in this material.

We would like to thank Mintu Mondal for his help in collecting the M-H data and Vivas Bagwe and John Jesudasan for technical help.

*Present address: Department of Physics and Astronomy, Northwestern University, 2145 Sheridan Road, Evanston, IL 60208, USA.
†pratap@tifr.res.in

[1] P. Szabo, P. Samuely, J. Kacmarcik, T. Klein, J. Marcus, D. Fruchart, S. Miraglia, C. Marcenat, and A. G. M. Jansen, Phys. Rev. Lett. **87**, 137005 (2001); M. Iavarone, G. Karapetrov, A. E. Koshelev, W. K. Kwok, G. W. Crabtree, D. G. Hinks, W. N. Kang, Eun-Mi Choi, Hyun Jung Kim, Hyeong-Jin Kim, and S. I. Lee, *ibid.* **89**, 187002 (2002); R. S. Gonnelli, D. Daghero, G. A. Ummarino, V. A. Stepanov, J. Jun, S. M. Kazakov, and J. Karpinski, *ibid.* **89**, 247004 (2002).
[2] M. Tinkham, *Introduction to Superconductivity* (McGraw-Hill, New York, 1996).
[3] P. W. Anderson, J. Phys. Chem. Solids **11**, 26 (1959).
[4] A. Gurevich, Phys. Rev. B **67**, 184515 (2003).
[5] L. Min-Xia and G. Zi-Zhao, Chin. Phys. **16**, 826 (2007).
[6] R. Nagarajan, C. Mazumdar, Z. Hossain, S. K. Dhar, K. V. Gopalakrishnan, L. C. Gupta, C. Godart, B. D. Padalia, and R. Vijayaraghavan, Phys. Rev. Lett. **72**, 274 (1994); T. Siegrist, H. W. Zandbergen, R. J. Cava, J. J. Krajewski, and W. F. Peck, Jr., Nature (London) **367**, 254 (1994).
[7] K. Izawa, K. Kamata, Y. Nakajima, Y. Matsuda, T. Watanabe, M. Nohara, H. Takagi, P. Thalmeier, and K. Maki, Phys. Rev. Lett. **89**, 137006 (2002); T. Park, M. B. Salamon, E. M. Choi, H. J. Kim, and S. I. Lee, *ibid.* **90**, 177001 (2003).
[8] P. Raychaudhuri, D. Jaiswal-Nagar, G. Sheet, S. Ramakrishnan, and H. Takeya, Phys. Rev. Lett. **93**, 156802 (2004).
[9] T. Yokoya, T. Kiss, T. Watanabe, S. Shin, M. Nohara, H. Takagi, and T. Oguchi, Phys. Rev. Lett. **85**, 4952 (2000).
[10] S. V. Shulga, S.-L. Drechsler, G. Fuchs, K.-H. Müller, K. Winzer, M. Heinecke, and K. Krug, Phys. Rev. Lett. **80**, 1730 (1998).
[11] M. Yethiraj, D. McK. Paul, C. V. Tomy, and J. R. Thompson, Phys. Rev. B **58**, R14767 (1998).
[12] S. Mukhopadhyay, G. Sheet, P. Raychaudhuri, and H. Takeya, Phys. Rev. B **72**, 014545 (2005).
[13] S. L. Drechsler *et al.*, Physica C **364-365**, 31 (2001); **317-318**, 117 (1999).
[14] See EPAPS Document No. E-PRBMDO-79-030913, section I, for details on the structural properties. For more information on EPAPS, see http://www.aip.org/pubservs/epaps.html
[15] Mark J. Higgins and S. Bhattacharya, Physica C **257**, 232 (1996).
[16] See EPAPS Document No. E-PRBMDO-79-030913, section II, for a detailed comparison of these two measurements (Ref. 14).
[17] H. Bitterlich, W. Löser, G. Behr, S.-L. Drechsler, K. Nenkov, G. Fuchs, K.-H. Müller, and L. Schultz, Phys. Rev. B **65**, 224416 (2002).
[18] γ_H in our undoped sample is larger than the value reported earlier in Ref. 17. However, their sample had a $T_c<15$ K and was therefore possibly in the dirty limit.
[19] The H_{c2} value for $H\|a$ in the undoped YNi_2B_2C sample was determined from isothermal M-H measurements.
[20] This is in qualitative agreement with the variation in H_{c2} reported in polycrystalline Pt-doped YNi_2B_2C samples; see G. Fuchs, K.-H. Muller, J. Freudenberger, K. Nenkov, S.-L. Drechsler, S. V. Shulga, D. Lipp, A. Gladun, T. Cichorek, and P. Gegenwart, Pramana, J. Phys. **58**, 791 (2002); G. Fuchs *et al.*, Physica C **408-410**, 107 (2004).
[21] In principle Ni and Pt have equal number of electrons outside the filled shell, e.g., Ni:$[Ar]3d^84s^2$ and Pt:$[Xe]4f^{14}5d^96s^1$. A significant change in $N(E_F)$ is therefore not expected.
[22] C. L. Huang, J.-Y. Lin, C. P. Sun, T. K. Lee, J. D. Kim, E. M. Choi, S. I. Lee, and H. D. Yang, Phys. Rev. B **73**, 012502 (2006).
[23] This result is in disagreement with Ref. 24 where a decrease in γ_n with Pt doping has been reported in samples of $YNi_{2-x}Pt_xB_2C$. We do not observe any decrease in γ_n with x in our samples.
[24] D. Lipp, M. Schneider, A. Gladun, S.-L. Drechsler, J. Freudenberger, G. Fuchs, K. Nenkov, K.-H. Muller, T. Cichorek, and P. Gegenwart, Europhys. Lett. **58**, 435 (2002); M. Nohara, M. Isshiki, F. Sakai, and H. Takagi, J. Phys. Soc. Jpn. **68**, 1078 (1999).
[25] H. Suhl, B. T. Matthias, and L. R. Walker, Phys. Rev. Lett. **3**, 552 (1959); E. J. Nicol and J. P. Carbotte, Phys. Rev. B **71**, 054501 (2005).